How to compute velocity-space tomographies using several fast-ion diagnostics

A.S. Jacobsen[1], M. Salewski[1], B. Geiger[2], M. García-Muñoz[3], W.W. Heidbrink[4], S.B. Korsholm[1], F. Leipold[1], J. Madsen[1] P.K. Michelsen[1], D. Moseev[2], S.K. Nielsen[1], J. Rasmussen[1], M. Stejner[1], G. Tardini[2] and the ASDEX Upgrade Team[2]

[1] *Association Euratom - DTU, Technical University of Denmark, Department of Physics - DTU Risø Campus, DK-4000 Roskilde, Denmark*

[2] *Association Euratom - Max-Planck-Institut für Plasmaphysik, D-85748 Garching, Germany*

[3] *Universidad de Sevilla, 41004 Seville, Spain*

[4] *University of California, Irvine, California 92697, USA*

Introduction

ASDEX Upgrade and LHD are equipped with collective Thomson scattering (CTS) [1–4] and fast-ion D_α (FIDA) [5, 6] diagnostics (or rather H_α in the case of LHD). These diagnostics measure fast ions in small volumes compared with the plasma size. In either diagnostic one pre-selects a viewing direction through geometric arrangement of the experiment and measures a 1D function, g, of the fast-ion 2D velocity-space distribution function f. In principle three FIDA views and two CTS views are available at ASDEX Upgrade, and two additional FIDA views are likely going to be installed in 2013. In the next ASDEX Upgrade campaign, seven views are thus expected to be available. Here we investigate the five-view FIDA system and the seven-view combined system through the use of synthetic measurements. Traditionally, fast-ion CTS or FIDA measurements are compared with simulated spectra to investigate whether the measurements match the expectation [1, 7, 8]. However, if the real measurements disagree with the synthetic measurements, it is often unclear what caused this discrepancy. Our final goal is to experimentally determine f, and this might help establish where in 2D velocity space the measurements disagree with the theoretical prediction. Inference of velocity-space tomographies from CTS or FIDA measurements was recently shown to be an achievable goal [9, 10]. We developed methods to account for uncertainty in the measurements which allow the use of CTS and FIDA measurements together to compute a joint velocity-space tomography [11]. Applying our prescription to a set of real 1D fast-ion measurements will yield an entirely experimentally determined 2D fast-ion velocity distribution.

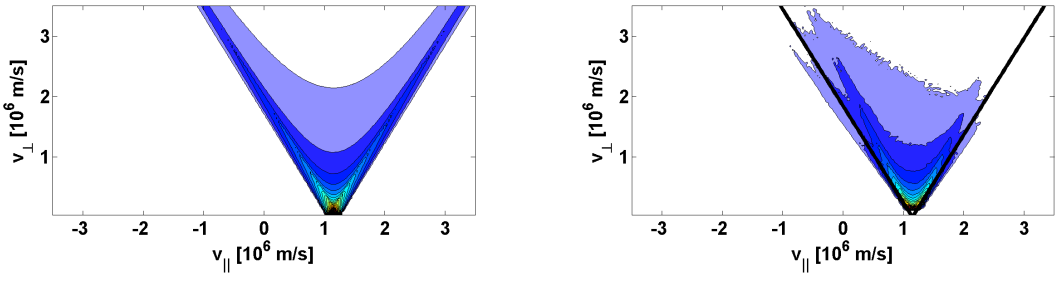

(a) CTS weight function.

(b) FIDA weight function shown together with the outline of the CTS weight function (black lines).

Figure 1: Weight functions for CTS and FIDA for a projection angle of 32°. The ranges of the projected velocity, u, for the CTS weight function, and the wavelength, λ, for the FIDA weight function are chosen such that the weight functions are as similar as possible.

Tomography of a velocity distribution function using a combination of diagnostics

Figure 1 shows weight functions for both CTS and FIDA for a viewing angle, ϕ, of 32°. The viewing angle is the angle between the magnetic field and the direction along which the velocity distribution of the fast ion is resolved. Weight functions relate the 2D fast-ion velocity distribution function f to the 1D measurements g and are essential components of our developed tomography procedure [9–11]. The CTS weight function shown in figure 1(a) is calculated analytically [9]. The FIDA weight function shown in figure 1(b) cannot be calculated analytically and so is calculated numerically. The FIDA weight function takes into account Stark splitting, the charge-exchange reaction probability, the probability of the n=3 to n=2 electron transition and instrumental effects in addition to the Doppler shift of the radiation. Figure 1(b) also shows the outline of the CTS weight function, illustrated by the black lines, to ease the comparison of the two weight functions. It is clearly seen that CTS weight functions are symmetric whereas the FIDA weight functions are asymmetric due to the effects of the charge-exchange probability. The slope of the outline of the FIDA weight function is furthermore slightly different compared to that of the CTS weight function due to the Stark splitting [11].

Figure 2 shows a typical ASDEX Upgrade fast-ion distribution function and two tomographic reconstructions. The distribution function shown in figure 2(a) is simulated using TRANSP and NUBEAM [12]. It shows maxima at full and half injection energy (60 keV and 30 keV) of neutral beam injector S3 at ASDEX Upgrade. The tomographic reconstructions are made using synthetic measurements calculated from the TRANSP simulation. Previously we used different

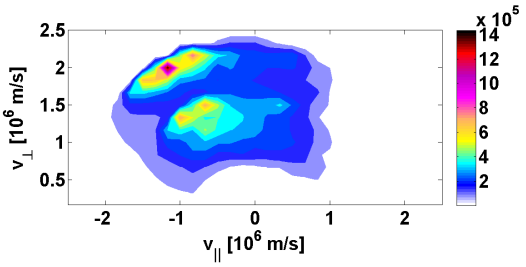

(a) Central fast-ion velocity distribution function typical for a low density discharge without mode-activity simulated using TRANSP/NUBEAM.

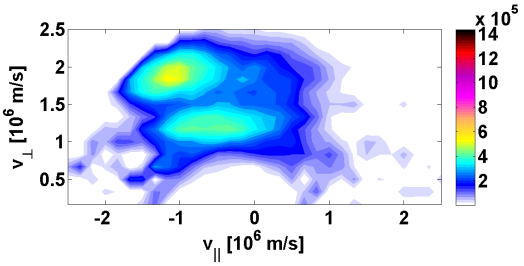

(b) Reconstruction of the distribution function using five synthetic FIDA views containing 5% noise.

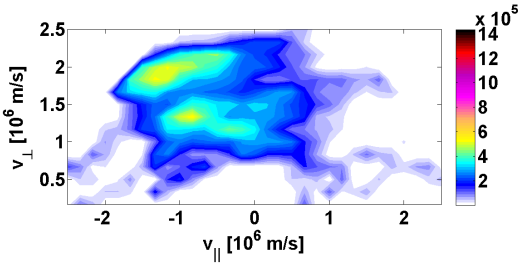

(c) Reconstruction of the distribution function using five synthetic FIDA views combined with two synthetic CTS views containing 5% noise.

Figure 2: A TRANSP/NUBEAM simulated fast ion velocity space distribution function and tomographic reconstructions of this. The unit of the colorbar is [s^2/m^5]. The tomographic reconstructions are made using synthetic measurements from five and seven views respectively.

grids for the original function and the tomography which added numerical noise. Here we use identical grids (31×15) but add 5% Gaussian noise to the measurements. The noise makes an accurate reconstruction of fine details impossible. Figure 2(b) shows a tomography using synthetic measurements from five FIDA views. For each view, the part of the spectrum that would be obscured in a real experiment due to beam emission and halo emission is omitted. Three of the chosen viewing angles are the angles of the three existing FIDA views at ASDEX Upgrade, which are here 11°, 21° and 67°. The remaining two viewing angles are 42° and 83°. It is seen how the overall shape of the distribution reappears in the tomography together with the two beam injection maxima. However, the 30 keV maximum is located further to the

right than in the simulation. Figure 2(c) shows the tomography using synthetic measurements from the five FIDA views combined with two CTS views. This system thus simulates the actual views expected to be available at ASDEX Upgrade during the next experimental campaign. The viewing angles for the CTS views are chosen to be 73° and 79° which are realistic angles. The part of the spectrum in the CTS measurements that would be obscured by bulk ions are omitted. Each FIDA and CTS view contains about 100 measurements. By comparing figures 2(b) and 2(c) it is seen that the tomography improves when a combination of FIDA views and CTS views are used. Both the peak intensity and the locations of the two beam injection maxima are better resolved in the tomography using a combination of views.

Conclusions

Tomographic reconstructions using five synthetic FIDA views and a combination of five synthetic FIDA views and two synthetic CTS views are inferred. It is seen that the tomography improves when a combination of FIDA and CTS is used compared to the tomography inferred only from FIDA views.

Acknowledgements

This work, supported by the European Communities under the contract of Association between Euratom and DTU, was partly carried out within the framework of the European Fusion Development Agreement. The views and opinions expressed herein do not necessarily reflect those of the European Commission.

References

[1] M. Salewski et al, Nuclear Fusion **50**, 035012 (2010)

[2] F. Meo et al, Journal of Physics: Conference Series **227** 012010 (2010)

[3] M. Nishiura et al, Review of Scientific Instruments **79**, 10E731 (2008)

[4] S. Kubo et al, Review of Scientific Instruments **81**, 10D535 (2010)

[5] B. Geiger et al, Plasma Physics and Controlled Fusion **53**, 065010 (2011)

[6] T. Ito et al, Plasma and Fusion Research **5**, S2099 (2010)

[7] W. W. Heidbrink et al, Plasma Physics and Controlled Fusion **49**, 1457-1475 (2007)

[8] W. W. Heidbrink, Review of Scientific Instruments **81**, 10D727 (2010)

[9] M. Salewski et al, Nuclear Fusion **51**, 083014 (2011)

[10] M. Salewski et al, Nuclear Fusion **52**, 103008 (2012)

[11] M. Salewski et al, Nuclear Fusion **53**, 063019 (2013)

[12] A. Pankin et al, Computer Physics Communications **159**, 157-184 (2004)